RESULTS OF THERMAL VACUUM TESTS FOR THE PASP+ FLIGHT MODULES

Henry Curtis[1], Don Guidice[2], Paul Severance[2], and Michael Piszczor[1]

1) NASA Lewis Research Center
2) Phillips Lab, Geophysics Directorate

INTRODUCTION

The PASP PLUS (Photovoltaic Array Space Power Plus Diagnostics) program is a photovoltaic experiment which will be flown on the Air Force satellite APEX (Advanced Photovoltaic And Electronic Experiment). APEX will be launched with a Pegasus during the summer of 1993. There are two other small experiments on APEX but PASP+ is the largest, uses the most power and accounts for over 90% of the data requirements. The orbit is elliptical with apogee and perigee of 1050 and 190 nautical miles respectively. The inclination is 70 degrees. The two main objectives of PASP+ are to determine the interactions between high voltage arrays and the space plasma environment and to determine the radiation damage characteristics of several newer types of solar cells.

In order to determine the interactions with the space plasma, several of the individual cell strings will be biased to voltages up to plus or minus 500 V, and leakage currents and arcing rates will be measured. The radiation degradation characteristics will be determined by the continuous monitoring of I-V data for all of the cell strings. As part of an overall testing program, the PASP+ panels and controller were put through a thermal vacuum test in order to check the thermal analysis, obtain temperature coefficients for the individual modules, and have an end-to-end test of the entire PASP+ experiment. This paper will describe briefly this thermal vacuum test and discuss the results obtained during that testing.

PASP+ DESCRIPTION

The PASP+ experiment consists of twelve photovoltaic modules with sixteen separate cell strings. Table I lists the sixteen different cell strings. There are a wide variety of cell types as well as two concentrator modules. Among the different cell types are silicon, GaAs on germanium substrates, InP, amorphous silicon, and three multi- bandgap cells, AlGaAs/GaAs, GaAs/GaSb, and GaAs/CIS.

As noted in Table I, not all of the individual modules will be biased for plasma interaction effects. Six of the individual modules will never be biased and only their radiation degradation will be measured. There are three modules with two or three individual strings. #'s 0, 1, and 2 are all 2x4 cm older silicon cell strings on the same module, while #'s 4 and 6 are GaAs strings on the same module. The other module with two strings is the GaAs/CIS module with two mechanically stacked multi-bandgap cell strings. Eight of the

Table I PASP+ Individual Cell Strings.

PASP+ #	Cell Type	Array Type	Bias	Cells
0	Silicon 2x4 cm	Planar	No	20
1	Silicon 2x4 cm	Planar	Yes	20
2	Silicon 2x4 cm	Planar	Yes	60
3	Silicon 8x8 cm	Space Station	Yes	4
5	Silicon 2.6x5 cm	APSA	Yes	12
4	GaAs 4x4 cm	Planar	Yes	20
6	GaAs 4x4 cm	Planar	Yes	12
8	GaAs 4x4 cm WT	Planar	Yes	4
11	GaAs 4x4 cm	Planar	Yes	8
10	InP 2x2 cm	Planar	No	10
9	Amorphous Si 4x4 cm	Planar	No	1
7	AlGaAs/GaAs	Planar	No	20
12	GaAs/CIS 2x2 cm	Planar	No	9
13	GaAs/CIS 2x4 cm	Planar	No	3
14	GaAs concentrator	Cassegrainian	Yes	8
15	GaAs/GaSb	Mini-dome Concentrator	Yes	12

individual strings are on a deployed panel (#'s 0-7), while the others are on the top surface of the APEX spacecraft.

Along with the photovoltaic modules, PASP+ has several diagnostic instruments to measure the environment or help determine the plasma interactions with the biased arrays. A Langmuir probe will be used to measure plasma properties; A dosimeter will measure the radiation environment in several energy bands; and a quartz crystal balance will be used to determine any contamination. A transient pulse monitor, an electrostatic analyzer and an electron emitter will be used in the plasma interaction portions of the experiment.

The last major portion of the PASP+ experiment is the controller, which will measure all the I-V curves, control the plus or minus bias voltages to the arrays, and in general run the experiment.

THERMAL VACUUM TEST DESCRIPTION

The thermal vacuum test was performed at the Boeing facility in Kent Washington during late June and early July of 1992. The work was supported by NASA contract NAS3-26604. The work was divided into three separate tests due to size limitations. The area covered by the solar simulator beam was not large enough to illuminate the entire PASP+ experiment, or even the deployed panel. Hence the first two tests were with the right half then the left half of the deployed panel illuminated, while the third test was with the payload shelf illuminated. During each test, only the panel being tested was in the chamber. In the two tests with the deployed panel, the half of the panel which was not being illuminated by the solar simulator was maintained at the required temperatures by a set of lamp banks built into the test support fixture.

Each of the three separate tests included the following:

1) A thermal balance cycle to determine the hot and cold operating temperatures.

2) Three thermal soak cycles at temperatures of 10 degrees higher than the hot operating temperature and 10 degrees lower than the cold operating temperature. The dwell time at each hot and cold tempera-ture was 90 minutes.

3) Eight thermal cycles between the operating temperatures with no dwell time. (Four cycles for each of the deployed panel tests).

During each of the three tests, chamber pressure was maintained near 10^{-7} torr. The solar simulator irradiance was monitored with blackbody detectors (water cooled) in the chamber. Between the first and second and between the second and third tests, the solar simulator irradiance was measured (in air) at the test plane with three reference cells. The reference cells were silicon, GaAs, and InP. The Isc was measured to calibrate the flux detectors while the Voc was measured as a temperature sensor to adjust the reference cell Isc data. The test fixture also included lamp banks to simulate the earth's albedo.

Each of the PASP+ modules has an RTD platinum temperature sensor. These were continuously monitored by the PASP+ controller. Several thermocouples were also added to the panel structure to monitor temperatures during the tests. These thermo-couples were continuously monitored by the Boeing test instrumentation. Since each of the modules could obtain different temperatures at different rates, there was one panel thermocouple designated to indicate when the simulator and lamp banks should be turned off and on. During the tests, the controller was in the test chamber and it was maintained near room temperature with auxiliary heaters.

During each of the three tests, between 40 and 50 I-V curves were taken for each of the modules under test. This data was stored in a small computer which was connected to the controller. The computer was in the main control room, which allowed near immediate viewing of the I-V data. The controller also continuously monitored the module temperatures, and displayed them in real time. The data was analyzed later at either NASA Lewis Research Center or Phillips Lab at Hanscom AFB.

MODULE TEMPERATURES

Figure 1 shows the temperature for the module which had the three silicon cell strings (#'s 0, 1, & 2). This data is typical for all the modules in all three tests. We first reached a hot temperature equilibrium, then turned the solar simulator off and waited 30 minutes for a cold temperature. 30 minutes was chosen because this is the longest expected eclipse during the PASP+ flight. After the thermal balance determination we did the hot and cold temperature soaks followed by the either four or eight rapid temperature cycles.

The data in figure 2 is just the thermal balance portion of the data in figure 1. Note the hot equilibrium temperature obtained after about 50 minutes and the 30 minutes of cooling before the simulator was turned back on. This data is typical of most of the PASP+ modules with ordinary thermal masses. Figure 3 shows the thermal balance portion for the APSA module, a very low thermal mass array. Note that the hot temperature equilibrium is reached in about three to four minutes and a cold balance temperature is reached in about 10 minutes. APSA is one of two low thermal mass modules on PASP+, the other one being the Space Station module. Table II shows the thermal balance temperatures for each of the PASP+ modules.

Table II Hot & Cold Thermal Balance Temperatures.

PASP+ #	Cell Type	Hot Temp	Cold Temp.
0, 1, 2	Silicon	44.4C	-57.7C
3	Silicon	62.7	-88.6
4, 6	GaAs	59.8	-43.0
5	Silicon	64.3	-85.8
7	AlGaAs/GaAs	35.2	-47.9
8	GaAs WT	37.9	-55.2
9	Amorphous Si	36.3	-36.8
10	InP	45.7	-35.0
11	GaAs	42.0	-54.2
12,13	GaAs/CIS	40.2	-36.8
14	GaAs Conc.	46.1	-21.8
15	GaAs/GaSb Conc.	49.4	-50.3

The Cassegrainian concentrator (#14) has a high thermal mass and after 30 minutes of simulated eclipse, the temperature dropped to only -21.8C. All the other modules had reached a cold equilibrium temperature after 30 minutes. During the 90 minute cold soaks however, the Cassegrainian reached a final cold temperature near -55C.

In general, the measured thermal balance temperatures offer no major surprises. Comparison with the predicted temperature from the thermal analysis is ongoing. After the three temperature soaks and the eight rapid temperature cycles, there was no measurable degradation in any module due to the thermal vacuum test.

MODULE ELECTRICAL PERFORMANCE

During each of the three thermal vacuum tests, between 40 and 50 I-V curves were taken for each module in that particular test. Sometimes, immediately after turning on the simulator after a cold soak, we would take a series of I-V curves to obtain data as the temperature changed. Hence, for each module, we have a collection of performance data at a wide variety of temperatures. From this data, we can generate plots of Isc, Voc, Pmax, and fillfactor vs. temperature and eventually, from straight line curve fits, determine the temperature coefficients.

Figures 4 and 5 are representative of the bulk of the electrical performance data. Figure 4 shows short-circuit current vs. temperature for module #0, a silicon module, while figure 5 shows open circuit voltage vs. temperature for the InP module #10. In both cases, the data is well represented by a straight line curve fit, leading to meaningful temperature coefficients. Table III lists the Isc, Voc, & Pmax temperature coefficients for each of the planar PASP+ modules in units of %/K. The temperature coefficients for the two concentrator modules are not included due to some data inconsistencies. The Cassegrainian module had a loose interconnection which changed the data from time to time. Since each element of the Cassegrainian has its own bypass diode, I-V data was always available. The mini-dome concentrator module showed a very large change in current with temperature and will be discussed later. There is no Isc data for the Space Station module due to an incorrect current sensing resistor in the controller. This has been replaced and we will be able to measure all the currents during the PASP+ flight.

In Table III, the modules are grouped into cell types. The first group of five modules are all made with silicon cells, while the second group of four modules are all made with GaAs cells. The last group contains the multi-junction cells and the third group contains the InP and the amorphous silicon modules. Note the silicon modules, as expected degrade faster with temperature than the GaAs modules, due mainly to a

higher percentage Voc degradation. The InP module has intermediate Pmax and Voc temperature coefficients, again as expected due to its individual cell Voc being between silicon and GaAs.

Table III PASP+ Module Temperature Coefficients (%/K)

Module		Isc	Voc	Pmax
0	Silicon	0.055	-0.359	-0.410
1	Silicon	0.058	-0.362	-0.404
2	Silicon	0.054	-0.357	-0.439
3	Space Station	------	-0.315	-0.403
5	APSA	0.042	-0.314	-0.431
4	GaAs	0.029	-0.198	-0.226
6	GaAs	0.024	-0.173	-0.179
8	GaAs WT	0.038	-0.176	-0.135
11	GaAs	0.036	-0.179	-0.204
10	InP	0.028	-0.235	-0.295
9	Amorphous Si	0.149	-0.246	+0.339
7	AlGaAs/GaAs	0.122	-0.216	-0.145
12	GaAs/CIS	0.031	-0.214	-0.312
13	GaAs/CIS	0.031	-0.201	-0.229

The most noteworthy temperature coefficients are for the multi-junction cell modules and the amorphous silicon module, which actually is a multi-junction cell. It had been expected that multi-junction cells would degrade faster than single junction cells due to the multiple voltage drops. However the GaAs/CIS modules have a lower degradation with temperature than silicon, and only slightly more than single junction GaAs. This is due mainly to the relatively low drop in Voc with temperature. These cells are also connected somewhat differently than conventional monolithic multi-junction cells. For instance, the basic building block for module #12 is three CIS cells in series which are in parallel with three parallel GaAs cells. Module #13 is similar except the ratio is 4:1 rather than 3:1.

Figure 6 shows the maximum power for the AlGaAs/GaAs monolithic multi-junction cell module (#7) vs. temperature. Note that the power decreases with increasing temperature for temperatures above 0C. For this portion of the curve, the Pmax temperature coefficient (shown in Table III), is quite low, at -0.145%/C. Below 0C, the power increases with increasing temperature. The low Pmax temperature coefficient is the result of the relatively large Isc positive temperature coefficient, 0.122%/C, which is twice as large as any other PASP+ Isc temperature coefficient except amorphous silicon. The change in Pmax at 0C is reflected in the fillfactor as shown in figure 7. Note that the fillfactor decreases significantly as the temperature decreases below 0C.

This change in both Pmax and fillfactor behavior at 0C has two possible explanations, both dealing with the change in bandgap of the two cells (AlGaAs & GaAs) with temperature. The first explanation is that as the bandgaps change with temperature, the monolithic cell matching currents become mismatched and affect the fillfactor and Pmax. The second explanation is similar except the changing bandgaps could see different portions of a non-perfect solar simulator spectrum produced by high pressure xenon lamps. In either case, the actual flight data will determine if there is a real break in the Pmax vs. temperature curve for AlGaAs/GaAs multi-junction cells.

The amorphous silicon module (#9) also exhibits some interesting behavior. Figure 8 shows Pmax vs. temperature for the amorphous silicon module while figure 9 shows the fillfactor. The Pmax increases

dramatically with temperature while the fillfactor does the same. As noted in Table III, The Isc also increases rapidly with temperature. Since the amorphous silicon cell is a monolithic multi-junction cell, similar arguments concerning bandgap shifts with temperature and non perfect solar simulation discussed above also apply. Again the flight data will be the final deciding factor. Nonetheless, it should be noted that the maximum measured Pmax is near the operating temperature for the amorphous silicon module.

The I-V curves generated during the thermal vacuum tests are all fairly ordinary with the exception of the mini-dome concentrator. Figure 10 shows I-V curves for the mini-dome concentrator module at five temperatures covering the entire temperature range encountered during the test. The voltage portion of the curves is quite normal with the small decrease with increasing temperature. The current however shows a very large increase with temperature more than doubling in the temperature range of -49C to 59C. It is expected that the lenses got quite cold during the tests and along with the simulated solar irradiance not being collimated to 32 minutes they somewhat defocused the light. Again, we will have the flight data as a final check. At operating temperatures, the module had a normal performance and there were no effects due to the thermal cycling.

SUMMARY

A series of thermal vacuum tests were performed on the PASP+ modules and flight controller. Three thermal soaks for 90 minutes at 10 degrees beyond the measured hot and cold extreme temperatures were performed as well as 8 thermal cycles. There were no damaging effects of the test on any of the modules and a few problem areas with the controller were corrected. We obtained excellent performance data for each module as a function of temperature and temperature coefficients were calculated. Some non-predicted data were observed but on further analysis, plausible explanations were found. The experiment is ready for launch.

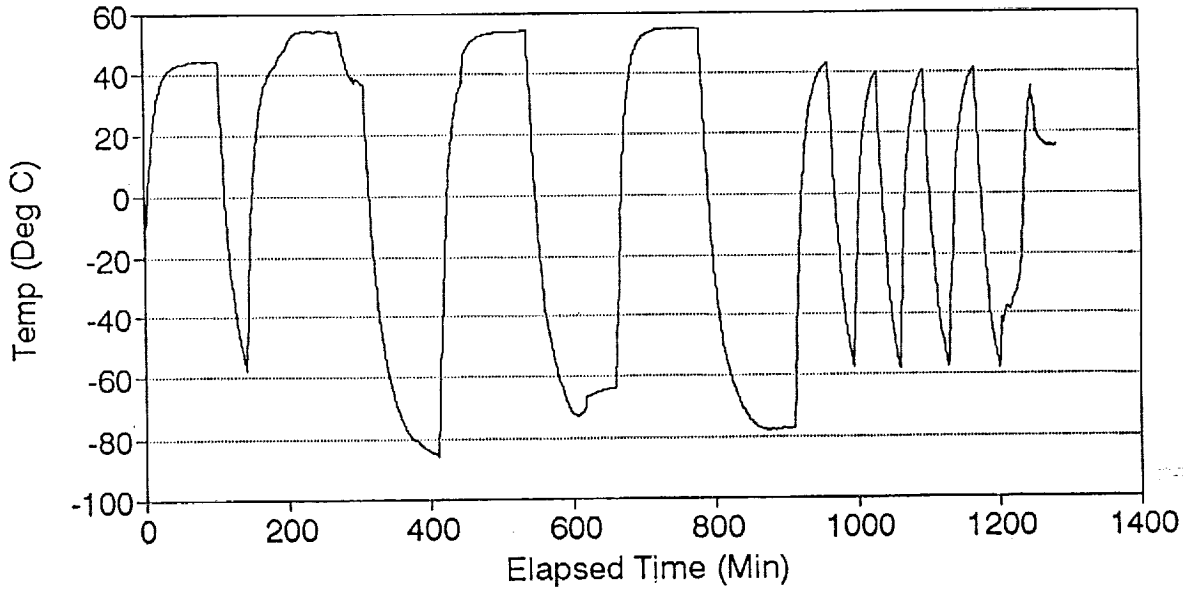

Figure 1. Temperature history for modules 0, 1, and 2, --- entire test.

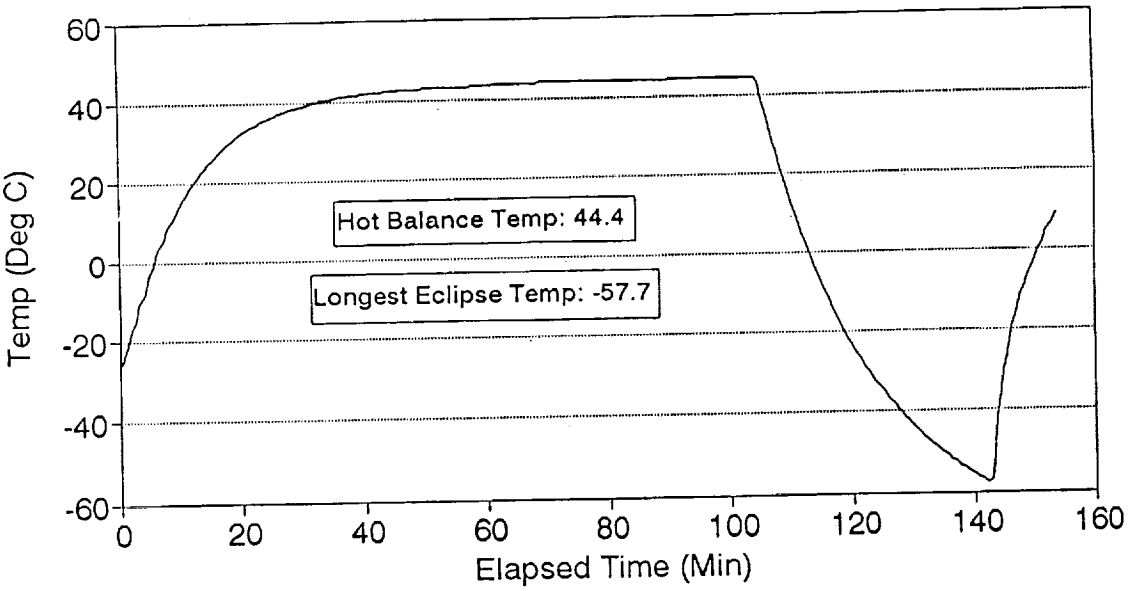

Figure 2. Temperature history for modules 0, 1, and 2, --- thermal balance.

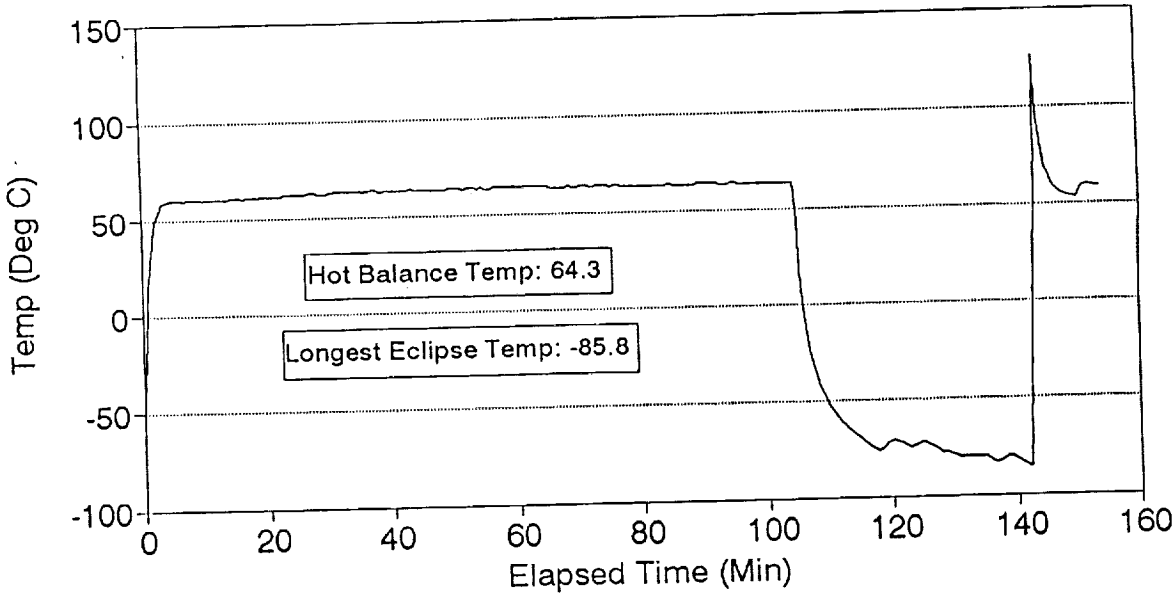

Figure 3. Temperature history for APSA module --- thermal balance.

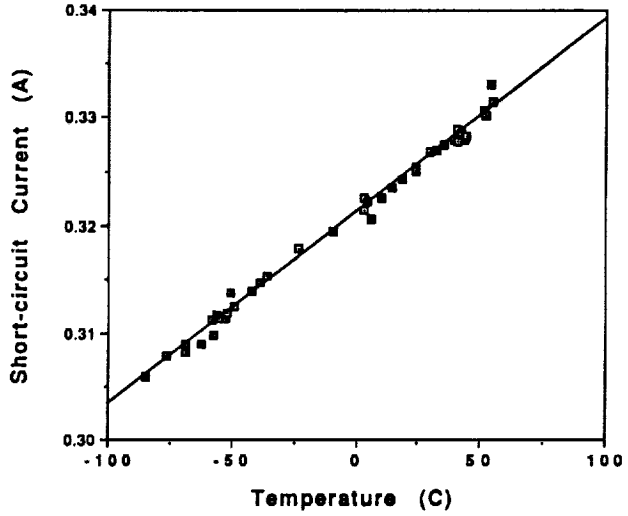

Figure 4. Short-circuit Current vs. Temperature for Module #0, Silicon.

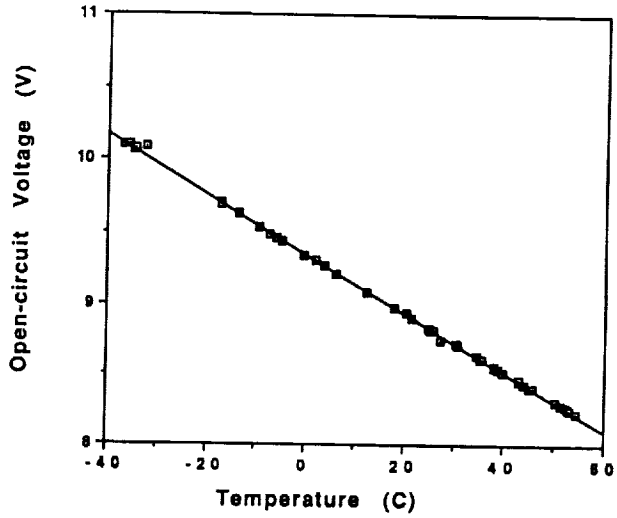

Figure 5. Open-circuit Voltage vs. Temperature for Module #10, InP.

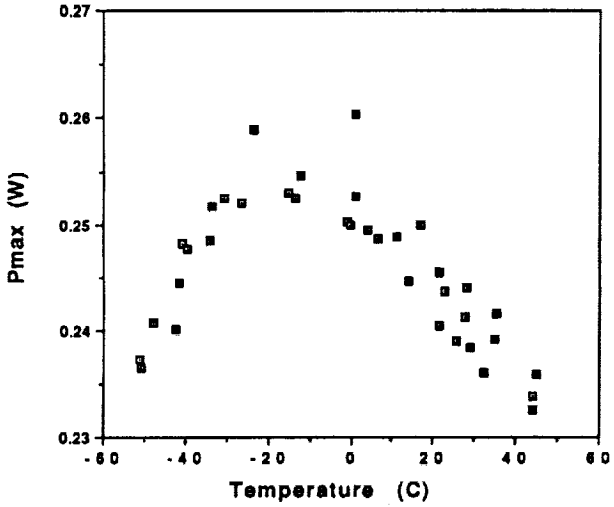

Figure 6. Maximum Power vs. Temperature for Module #7, AlGaAs/GaAs.

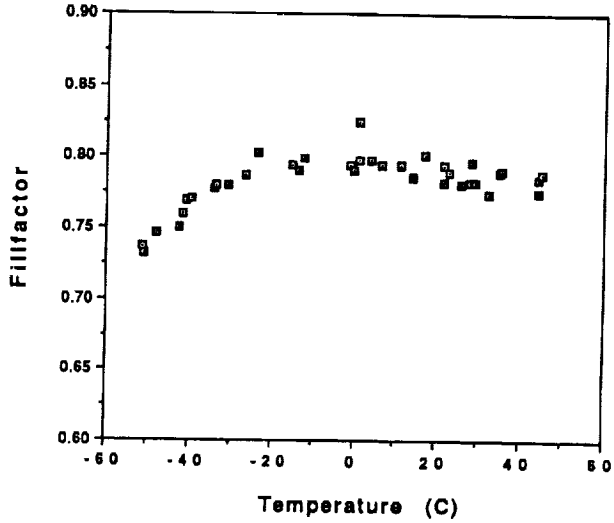

Figure 7. Fillfactor vs. Temperature for Module #7, AlGaAs/GaAs.

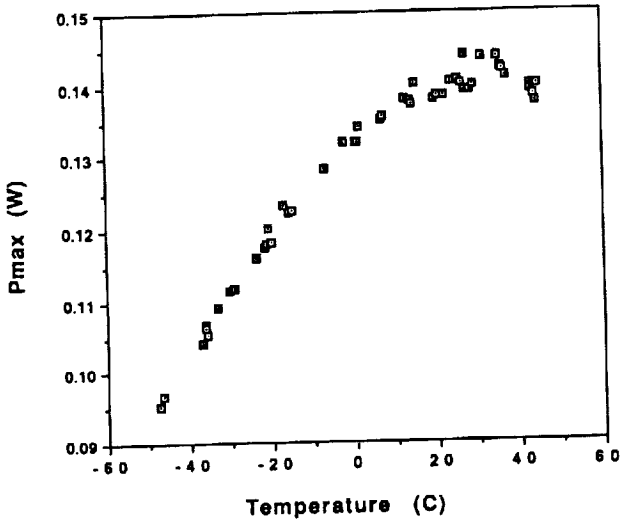

Figure 8. Maximum Power vs. Temperature for Module #9, Amorphous Si.

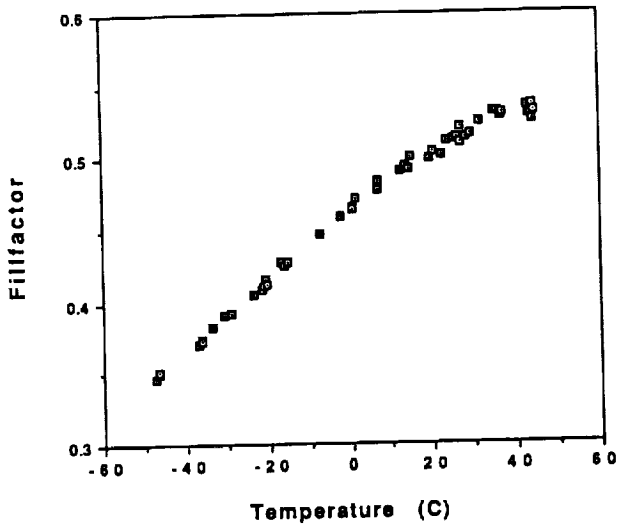

Figure 9. Fillfactor vs. Temperature for Module #9, Amorphous Si.

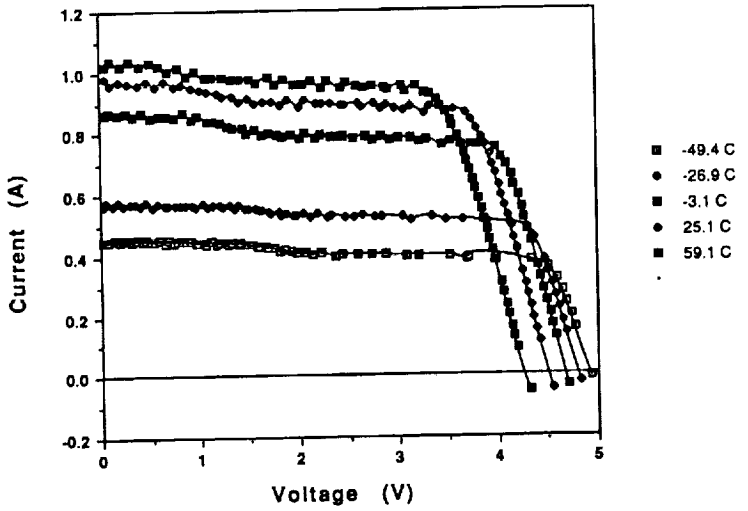

Figure 10. I-V Curves for Different Temperatures for Module #14, Mini-dome.